

1 **Article type:** Full length article

2 **TRL level:** 3

3 **Title**

4 Paper characteristics and their influence on the ability of Single Metal Deposition to
5 detect fingerprints

6 **Authors**

7 Ouahiba ACHERAR ^a

8 Minh Quang TRUONG ^b

9 Sylvain ROBERT ^{a *}

10 Frank CRISPINO ^{a, d}

11 Sébastien MORET ^{b, c (present address)}

12 Andy BÉCUE ^b

13 (*) corresponding author

14 **Affiliations**

15 ^a Laboratoire de recherche en criminalistique; Département de chimie, biochimie et
16 physique; Université du Québec à Trois-Rivières, QC, Canada, G9A 5H7

17 ^b École des sciences criminelles; Faculté de droit, des sciences criminelles et
18 d'administration publique; Bâtiment Batochime, Université de Lausanne, CH-1015
19 Lausanne-Dorigny, Switzerland

20 ^c University of Technology Sydney, Centre for Forensic Science, Broadway 2007,
21 Australia

22 ^d Centre international de criminologie comparée, Université du Québec à Trois-
23 Rivières, QC, Canada, G9A 5H7

24 **Email addresses**

25 Sylvain ROBERT (Sylvain.Robert@videotron.ca, Sylvain.Robert@uqtr.ca)

26 Frank CRISPINO (Frank.Crispino@uqtr.ca)

27 Sébastien MORET (Sebastien.Moret@uts.edu.au)

28 Andy BÉCUE (Andy.Becue@unil.ch)

29 **Abstract**

30 This study aims at exploring the way paper samples may impact the performance of Single-
31 Metal Deposition (SMD II), a fingerprint detection technique known for its versatility of
32 application as well as its sensitivity regarding porous substrates. To get a broader view on
33 how porous substrates may impact the SMD II performances, 74 North American and
34 European papers types were collected, characterized (UV-visible and infrared spectroscopy,
35 roughness, porosity, and surface pH), and processed as substrates bearing fingerprints. This
36 part of the study represented a first valuable outcome by the number of samples considered.
37 After processing with SMD II, the samples were characterized again with the techniques
38 mentioned above, background staining and fingerprint quality were assessed and associated
39 with a quality score. Overall, no positive nor negative trend was observed between the paper
40 characteristics and the SMD II performance. As a consequence, it is currently still not possible
41 to predict if a paper sample will behave well or bad with SMD II. Of all the monitored
42 parameters, the chemical composition of the surface coating (*i.e.*, silica or calcium carbonate)
43 may be worth exploring further, as it has been observed that some coatings undergo partial
44 degradation during the SMD II process. As a result, secretion residue may be damaged by
45 the chemical solubilization of the support layer if they failed to penetrate deeper into the
46 substrate.

47 **Keywords**

- 48 • Forensic Science
- 49 • Chemical analysis
- 50 • Porous substrate
- 51 • Surface properties
- 52 • Gold Nanoparticles

53

54

55

56

57 **Highlights**

- 58 • Physical surface topography (roughness and porosity) as well as cellulose and lignin
59 chemical groups have no detectable influence on fingerprints detection using the SMDII
60 technique
- 61 • The only factor that may be of importance seems to be the chemical composition of
62 surface coating (silicates and carbonates).

63

64 1. Introduction

65 1.1. Detection of fingermarks using single-metal deposition (SMDII)

66 Multimetal deposition (MMD) is a fingerprint detection technique based on the use of colloidal
67 gold. The application protocol is built along a two-step process: (i) a detection bath containing
68 gold nanoparticles which bind to secretion residue under specific conditions, followed by (ii) a
69 contrast reinforcement bath based on the selective reduction of metal on gold nanoparticles.
70 As a result, MMD-processed fingermarks appear as dark/light-grey ridges on a relatively
71 unstained substrate [1]. Initially named “The Universal Process” [2] for its ability to detect
72 marks on a wide range of substrates (e.g., porous, non-porous, semi-porous, adhesives), the
73 technique was proposed in 1989 [3] and has consistently been improved since, to make it
74 more reliable and user-friendly.

75 Amongst the various improvements, it is possible to cite the optimization of the colloidal gold
76 synthesis, by Schnetz, to obtain more homogenous (in size and shape) and smaller (from 30
77 to 14 nm) nanoparticles [4]. This led to MMD II. Another improvement of the technique
78 consisted in replacing the silver-on-gold reinforcement step by a gold-on-gold one [5,6], that
79 proved to produce the same quality of results, with more reliable outcomes, improved control
80 and cheaper costs. At this stage of development, the technique was renamed Single-Metal
81 Deposition (SMD). Finally, the colloidal gold synthesis was further optimized, as well as the
82 application protocol to make it more end-user friendly [7,8]. The latest evolution of the
83 technique, SMD II [8], is characterized by a modified colloidal gold synthesis and a simplified
84 application protocol (e.g., no pH monitoring). As a result, the gold deposition process is more
85 reliable and less pH dependent.

86 The key step of the technique (being MMD or SMD) remains the gold nanoparticles
87 deposition onto fingerprint residue, which is not yet fully understood despite the various
88 optimization and improvement steps. This is a major limiting factor as it makes it difficult to
89 cope with apparent unreliability when processing items or substrates. For example, the
90 technique can give very good results on problematic substrates, such as cling films [9], but
91 suffers from several issues on conventional substrates, such as paper [10]. Among the lack of
92 reproducibility and inconsistent detection performance observed on papers, it is possible to
93 cite: unexplained background staining that can diminish the contrast, unwanted deposition of

94 gold nanoparticles on the substrate instead of the ridges (reversed detection), or absence of
95 detection (null result). In order to fix those issues, a better understanding of the influence
96 papers may have on the SMD performance is consequently required.

97 The main objective of this study is to monitor the effect of the composition and structure of
98 different types of paper from North American and European markets on the detection
99 efficiency of SMD II. Spectrophotometric methods as well as paper physics properties
100 (surface pH, surface profilometry, roughness and porosity) were considered to identify the
101 parameters that may influence the quality of the detected fingermarks or induce unwanted
102 background staining. Such knowledge would help designing a more robust and efficient SMD
103 formulation, so that it can be reliable independently from the types of papers. Readers
104 interested in fingermark composition and detection can refer to the most recent publications in
105 the field, such as [11].

106 **1.2. Paper composition and properties**

107 **1.2.1 Paper chemical composition**

108 Wood represents the major raw material in the manufacture of paper, aside for specialty
109 papers using cotton or linen, or low grade papers using annual plants. The main constituents
110 of wood are cellulose, hemicelluloses and lignin (Figure 1). Other components, known under
111 the general term of extractives, are present in small and variable quantities. Two types of
112 wood can be distinguished: softwoods (coniferous) and hardwoods, differing mostly by their
113 content in lignin (*i.e.*, 25-35% and 18-25%, respectively). It can be noted that the lignin
114 content in tropical hardwoods may exceed that of many softwoods. Softwoods and
115 hardwoods share a similar amount of cellulose (40-50%), and varying structures and
116 quantities of hemicellulose [12].

117 < Insert Figure 1 here >

118 **1.2.2 Cellulose**

119 Cellulose is a polysaccharide consisting of a linear chain of several hundreds to many
120 thousands of $\beta(1\rightarrow4)$ linked D-glucose units. The cellulose macromolecules are organized in
121 a unit called an elemental microfibril (10 nm in width and 5 nm in thickness), in which there

122 are about 100 cellulosic polymers connected by intra- and inter-molecular hydrogen bonds.
123 The main characteristic of this polymer is its insolubility in water, which is the result of the very
124 high molecular mass (3000 glucose units).

125 **1.2.3 Hemicelluloses**

126 Hemicelluloses differ from cellulose by the degree of polymerization (150-200), and by the
127 branching of molecular chains (Figure 1, lower right). The constitutive sugars of
128 hemicelluloses are divided into four groups: pentoses, hexoses, hexuronic acids and
129 deoxyhexoses. These units are connected by (1→4) or (1→6) links [12].

130 **1.2.4 Lignin**

131 Lignin is a thermosetting polymer with a very strong aromatic character and a molecular
132 weight that may exceed 40,000 g.mol⁻¹. The main constituting unit is the phenylpropane,
133 linked by ether-carbon or carbon-carbon bonds [12]. Lignin ensures the cohesion of the fibers
134 between each other by acting as natural glue. The complexity of lignin is such that much
135 research is still under way to define its molecular structure in a much more precise way.
136 Figure 1 shows a model of the chemical structure of softwood lignin at the top of the figure.
137 Different wood species have different lignin structure and composition.

138 **1.2.5 Surface roughness**

139 Paper roughness is an important parameter for its physical characterization. It is therefore
140 essential to be able to quantify the roughness of a paper so that the given value correlates
141 with the expected use of this paper, for example printing. In our case, it would be interesting
142 to see if surface roughness can be correlated with the quality of affixing of the secretion
143 residue composing the fingermarks on the different types of paper.

144 Roughness is defined as the average distance between the paper surface and a reference
145 plane to be defined. The roughness indices increase with the roughness of the paper [13].
146 Various parameters such as Ra, Rq, Rt and Rz are defined to quantify the roughness of a
147 paper surface (Table 1). Rq is the value we will use in our analysis.

148 < Insert Table 1 here >

149 **1.2.5 Porosity**

150 Paper has a porous structure formed by a network of fibers. Accordingly, there is a two-phase
151 arrangement in which pores and voids between fibers form an important part of its structure
152 [14]. Paper porosity is correlated with several properties such as absorption, opacity, and ink-
153 paper interaction. The porosity is influenced by the processing conditions, the addition of
154 pigments and chemical additives. For some grades of paper, a coating is applied to the top
155 surface of the paper to change its porosity [15].

156 In forensic science, an appropriate fingerprint detection sequence is usually chosen by
157 associating the item to one of the main substrate classes: porous, non-porous or semi-porous
158 (if we exclude specific substrates such as adhesives, metals, etc.). These categories are
159 based on the apparent (empiric) porosity of the substrate, which is known to influence the
160 behavior of the secretion residue [11]. Office papers are associated with porous substrates,
161 while magazine papers are usually considered as semi-porous substrates.

162 **2. Material and Methods**

163 **2.1. Paper collection and characterization**

164 **2.1.1 Paper sampling**

165 74 different kinds of paper (e.g., inkjet, LaserJet, copier, envelope, newsprint, Offset, drawing,
166 artistic) from 70 to 275 g.m⁻² basis weight were used in this study (see Appendix A for
167 details). These paper samples originated from Europe (e.g., Germany, Austria, Finland,
168 France, Portugal, Sweden and Switzerland), Canada, Mexico, and United States of America.
169 The samples were characterized by a range of paper composition: sugar cane (95%),
170 cardboard, colored, recycled fibers (10, 20, 30, 50% and even 80% post-consumer fibers),
171 wheat, FSC (Forest Stewardship Council) approved, Kraft, bleached Kraft, bleached generic
172 and blended mixed FSC.

173 **2.1.2 UV-Visible-NIR spectroscopy**

174 UV-visible spectra were taken on a Varian/Agilent Cary 5000 UV-VIS-NIR spectrophotometer
175 equipped with a diffuse reflectance integrating sphere (350-850 nm for UV-Visible part and
176 4000-600 cm⁻¹ for IR). The choice of this method is necessary because paper is a solid,

177 strongly absorbent, and highly diffusive material. The main functional groups responsible for
178 the sensitivity to light of lignin are the carbonyl and phenolic groups, quinones and various
179 conjugated double bonds [12].

180 Ten spectra of each paper sample were recorded, averaged and analyzed using the
181 ACD/SpecManager™ version 12.00 from ACD/Labs (*Advanced Chemistry Development*)
182 software.

183 **2.1.3 Profilometry**

184 3D profiles of the paper surface were recorded with a contact free optical profilometer (Veeco
185 Wyko NT1100™ instrument) using a Mirau interferometer. Phase shift interference (PSI) and
186 vertical offset interference (VSI) can be used to respectively measure smooth and rough
187 surfaces (heights that can reach up to 1mm). Those two modes were used to optimize
188 detection and measurements of the paper samples.

189 **2.1.4 Porosity measurements**

190 Porosity measurements were carried out with a Parker Print Surf™ (PPS) device from
191 Hagerty Technologies™. The flow of a fluid (air in our case) that passes through the paper
192 was measured with a pressure of 1960 kPa.

193 **2.1.5 Surface pH measurements**

194 pH measurements were carried out with a pH Pencil from HYDRION™, measuring a gradient
195 of H₃O⁺ ions on the paper surface. The first step was to moisten the surface of the paper with
196 distilled water, then to mark a line with the pen. After 15 minutes, the color of the line was
197 compared with the shades of color (color sheet) accompanying the pen. Although this method
198 is not fully accurate, it is a good way to discriminate a wide range of surface pH otherwise
199 very difficult to measure, and as pH is the most critical parameter to control for SMD
200 development, it could be planned that such an easy semi-quantitative pH tester could be
201 deployed to assist practitioners.

202 **2.2. Fingermark collection**

203 Natural and sebum-rich marks from two donors were collected for this study. For the natural
204 fingermarks, the donors were asked not to wash their hands one hour prior deposition. No
205 intentional enrichment was performed before collecting the fingermarks. For the sebum-rich
206 marks, the donors rubbed their hands on their forehead before depositing the fingermarks.
207 One natural and one sebaceous-rich marks were collected in duplicate for each donor and
208 substrate. Fingermarks were left to age for one month in the dark. This aging period has been
209 chosen to avoid the processing of fresh marks (e.g., one-day-old or one-week-old marks) and
210 to focus on marks compatible with a casework timeline. Temperature and humidity were not
211 monitored, nor controlled.

212 **2.3. Fingermark detection, quality rating and background evaluation**

213 The paper samples bearing fingermarks were processed using the latest SMD II protocol [8]. .
214 Given that paper can modify the pH of the solution and have an adverse impact on the
215 results, the paper samples were cut so that they all weight the same mass. Each paper
216 sample was then processed in 200 ml of colloidal gold solution. Since the focus of the study is
217 to investigate the effect of the different types of paper on the SMD II performance, each paper
218 type was processed in a newly prepared bath of colloidal gold. After completion of the SMD II
219 protocol, the samples were left to dry before being scanned on an Epson Perfection V330
220 Photo™ at 1200 dpi, without any digital enhancement. Once scanned, each mark was rated
221 by three independent assessors using a scale ranging from 0 to 3 (Table 2 [16]).

222 SMD II is known to produce unwanted, uncontrolled and non-homogeneous darkening of the
223 porous substrate. In order to understand what parameters may trigger background staining,
224 the color of each paper was recorded before and after fingermark detection. Background
225 measurement was done as follows: for each paper type, an unprocessed sample was placed
226 next to a processed sample and photographed under a homogeneous lighting. Photographs
227 were taken in grey scale and the value of the color was extracted using the eyedropper tool
228 on Adobe Photoshop. Those values range from 0 (black) to 255 (white). For unprocessed
229 samples, one measurement was made in the center of the paper. Processed samples
230 required to conduct four measurements at four different locations which were then averaged,
231 to take background staining inhomogeneity into account. The obtained value was then
232 subtracted from the value of the unprocessed sample. A positive value means a darkening of
233 the substrate whereas a negative value means a lightening.

234 < Insert Table 2 here >

235 **2.4. Statistical Analysis**

236 In order to highlight the potential correlation between the results of SMD II and the different
237 analyses performed on paper samples, a data analysis was performed. As a first step, the
238 raw results were organized using a Microsoft Office Excel spreadsheet. The analytical part
239 was performed with the data processing software "R 3.0.2". The different methods of analysis
240 considered were (i) the chi-square test where each variable extracted from the paper
241 analyses was assessed against the results of SMD II (fingerprint quality and background
242 staining) and (ii) a joint analysis of variables using principal component analysis (PCA),
243 multiple correspondence analysis (MCA) and multiple linear regression (MLR).

244 **3. Results and Discussion**

245 **3.1 Paper characterization (before SMD II)**

246 **3.1.1 UV-Visible spectroscopy**

247 Figure 2 shows the processing of the UV-Visible spectrum obtained for the sample "C03".
248 Each processed spectrum represents the variation of the log of the inverse of the reflectance
249 as a function of wavelength.

250 < Insert Figure 2 here >

251 Figure 3 shows the UV-Visible spectra of some North American (C01 and C02) and European
252 (E21 and E31) samples. The spectra show absorptions in the UV-Visible region. These
253 absorptions are due to the presence of lignin and the colored products of the paper (dyes,
254 coating pigments).

255 < Insert Figure 3 here >

256 It is possible to deconvolute the spectra to identify the electronic transitions between the
257 various occupied molecular orbitals (OMO) and unoccupied molecular orbitals (UMO), if these
258 are involved in our study.

259 The 100 to 350 nm region has not been considered because of the intense background noise
260 cause by the presence of even a small amount of lignin. UV-Visible analysis of SMD II-
261 processed samples shows an increase in absorption for some of the papers and a decrease
262 for others.

263 The reduction in the intensity of absorption of the spectral bands can be explained by 1) the
264 oxidation of the chromophores during the SMD II process. This has led to the displacement of
265 the other bands at longer wavelengths, towards the red part of the spectra (bathochromic
266 effect) and 2) the breaking the double bonds and formation of new compounds by
267 modification of polarity. Other papers are characterized by hypochromic displacements to
268 shorter wavelengths (towards ultraviolet).

269 **3.1.2 IR spectroscopy**

270 The four most important infrared regions for cellulose are the region of the bound and free OH
271 elongations between 3660 and 3000 cm^{-1} , the region of the aliphatic CH elongations between
272 3000 and 2800 cm^{-1} , the region of elongations C-O alcohols (or a cyclic system) of between
273 1350 and 1000 cm^{-1} , as shown in Table 3.

274 IR analysis showed that the many bleached papers samples designed for printing purpose
275 contain very small amounts of lignin. We also observed that about 80% of the samples (apart
276 from photographic papers and some colored papers) possess a carbonate coating, mainly
277 because these papers are intended for printing.

278 Carbonate characteristic peaks are located between 2530-2500, 1815-1770, and 1490-
279 1370 cm^{-1} (CO_3^{2-} elongation band), 910-850 cm^{-1} (O-C-O deformation band), 885-870 cm^{-1}
280 and 715 cm^{-1} [17]. FTIR analysis of a calcium carbonate powder allowed the identification of
281 these bands and with the use of the ACD/SpecManager software, identification of these
282 bands in the paper samples was possible. This allowed subsequent verification of the
283 presence or loss of the carbonate layer after treatment with the SMDII.

284 < Insert Table 3 here >

285 **3.1.3 Profilometry and roughness**

286 The profilometry allowed obtaining the 3D topography of all paper samples (Figure 4). For
287 sample C01, which is a glossy white paper used for inkjet printing, a uniform surface has
288 been measured, with very low Rq ($0.068\pm 0.009\mu\text{m}$). This makes sense given that the surface
289 is coated with a layer of mineral pigments which makes the surface of this paper smoother
290 and brighter.

291 < Insert Figure 4 here >

292 Figure 5 shows the value and variation of the Rq values of North American and European
293 papers. The parameters Ra, Rq, Rt and Rz characterizing the roughness of each paper give
294 the same variation, whether for North American or European papers. Rq corresponds to the
295 quadratic mean value of the profile deviations. Rq values ranged from $0.07\pm 0.01\mu\text{m}$ to
296 $6.07\pm 0.01\mu\text{m}$ for papers from North America and from $3.1\pm 0.6\mu\text{m}$ to $4.5\pm 1.1\mu\text{m}$ for samples
297 from Europe. The standard deviations of the different measurements are high (Figure 5),
298 because the samples are not uniform at the microscopic level.

299 < Insert Figure 5 here >

300 **3.1.4 Porosity**

301 Figure 6 shows the variation in average airflow in mL/min of North American and European
302 samples. It can be noted that there is a very large variation in air flow, which makes it possible
303 to distinguish the most porous samples from less porous ones.

304 < Insert Figure 6 here >

305 We have attempted to find a relationship between surface roughness and porosity (Figure 7).
306 This analysis is presented as the variation of Rq as a function of the airflow rate. Our results
307 indicate that roughness and porosity of the paper are not correlated

308 < Insert Figure 7 here >

309 **3.1.5. Surface pH**

310 The values of surface pH reported for the tested paper samples can be found in Appendix A.
311 The majority of the tested papers have a neutral pH (82%), while only a few have a slightly
312 acidic (10%) or basic pH (3%). This result was expected since most of writing papers are

313 acid-free for document preservation purposes. Only three paper types have a pH of 4 or 5
314 (C01, C20, C41).

315 **3.2 Impact of SMD II on the paper properties**

316 **3.2.1 Carbonate-coated papers**

317 The IR spectra of carbonate-coated samples before and after the application of SMD II were
318 mathematically subtracted from each other and compared with the spectrum of calcium
319 carbonate. Figure 8 illustrates the results obtained for the paper sample RetroPlus50 Canada
320 (C02). It appears that the loss observed on the spectrum resulting from the subtraction “after-
321 before SMD II” (Figure 8 - top) could be correlated with the loss of calcium carbonate (Figure
322 8 - bottom).

323 < Insert Figure 8 here >

324 This loss can be explained by the fact that SMD II requires to immerse the papers in an acidic
325 solution (pH close to 3). IR analysis allows identifying the peaks of the different components
326 and hence estimate a loss of carbonate. However, the quantitative analysis must be
327 completed with chemical analysis to confirm the proportions of carbonates present. When
328 assessing the % of loss by looking at the carbonate absorption band, it appears that most of
329 the paper samples loose between 20 to 50% of this layer. Some papers undergo a total loss
330 (100%). One hypothesis could be that the detrimental effect that SMD II has on the carbonate
331 layer do have a direct impact on the detection performance. This hypothesis will be
332 investigated further in this contribution.

333 **3.2.2 Photographic papers**

334 It was not easy to determine the exact composition of the photographic papers with the IR
335 analyzes. Figure 9 shows the three IR spectra of the sample C01, the first spectrum at the top
336 shows the result of the subtraction between the spectra recorded before and after SMD II was
337 applied. What can be seen on this difference spectrum is that there is a loss of three bands
338 which are at 1721, 1653 and 1423 cm^{-1} and a band amplification at 1584 cm^{-1} which is
339 identifiable in the post-SMD II spectrum.

340 < Insert Figure 9 here >

341 The subtraction between the pre-SMD II spectrum of C01 and another sample, for example
342 C04 (for which we were able to determine its cellulose and carbonate composition) shows
343 that no peak corresponds to cellulose in the C01 spectrum, as shown in Figure 10. The
344 photographic coating layer is probably too thick for the infrared radiation to reach the inner
345 layers of the paper. All the photographic papers collected in this study are also coated with
346 silicate, as shown in our FTIR spectra.

347 < Insert Figure 10 here >

348 Silicate in its various forms (gel, precipitate or colloidal) is the most widely used pigment for
349 the coating of photographic paper to provide a smooth and shiny surface [18]. The most
350 characteristic peaks of silicate are shown in Table 4 [19,20,21]. All photographic samples
351 considered in this study have a silicate coating. The positions of the spectral bands depends
352 on the type of silica used, as well as on the way the coating recipe is prepared (temperature,
353 solvent used, etc.).

354 < Insert Table 4 here >

355 Post-SMD II IR analysis showed that there was no change at the surface of the photographic
356 paper, and therefore no loss of this layer. This can be explained by the fact that the silica
357 layer is quite thick and that it remains stable at acidic pH (no dissolution of this layer). In
358 reference [18], the author describes the factors influencing the dissolution of amorphous
359 silica. Among these factors, the pH has a limited role as the dissolution is almost negligible for
360 pH below 3 and above 9. Finally, the infrared analysis did not allow the determination of the
361 type (or composition) of silica used for the coating of the photographic papers considered in
362 this study.

363 **3.2.3 Colored papers**

364 Some colored papers are coated with carbonate (C03, C08, C32, E30, E31, E32), while
365 others contain very little or no carbonate, such as C23 and C27 (all colors), E27, E28 and
366 E29. For the sample C27, IR analysis shows the presence of cellulose (Figure 11). The other
367 peaks belong to the aromatic compounds present (CH aromatic elongation 3083, 3060,
368 3026 cm^{-1} , elongation C=O 1730 and 1704 cm^{-1} , CC elongation of the aromatic ring at 1601,
369 1493, 1452 cm^{-1} , out-of-plane deformation CH aromatic at 697 cm^{-1}).

370 For the post-SMD II IR spectrum for sample C23 (with all colors), the intensity of certain
371 bands (1468 and 1445 and 853 cm^{-1}) decreased, while the intensity of other bands increased
372 (1731, 1155 cm^{-1}). The difference between the spectra obtained before and after SMD II
373 emphasizes this decrease but no loss of spectral bands. This is also true for sample C27.

374 < Insert Figure 11 here >

375 Several paper samples (C10, C33, C37, C40, E08, E11, E16, E18, E19, E20, E21, E22, E27
376 E28, E29 E31, E30, E32) showed spectral band losses at 3340-3350 cm^{-1} and at 2920 cm^{-1} .
377 Probably it is the $\text{CH}_2\text{-OH}$ group of the cellulose which is lost during the treatment with SMD II
378 (protonation of the alcohol in an acidic medium). The calculation of the derivative with the
379 ACD/SpecManager software made it possible to identify the IR bands corresponding to the
380 carbonate and the cellulose. The band at 711 cm^{-1} is identified in the carbonate with an
381 accuracy of $\pm 1 \text{ cm}^{-1}$. This band is used to calculate the amount of carbonate lost during the
382 processing with SMD II (this band is easily identifiable) (Figure 12).

383 < Insert Figure 12 here >

384 **3.4 Correlation between the SMD II performance and the paper characteristics**

385 Overall, 592 fingerprint samples were processed and assessed throughout the study, leading
386 to fingerprints detected with scores ranging from 0 to 3. As expected, the technique also led
387 to background noise inducing a darkening of the paper surface for most paper types. The
388 colored papers presented a lightening of the color, most certainly due to the successive water
389 baths of the SMD II protocol.

390 The quality scores that have been associated with the detected fingerprints are
391 representative of the performance of SMD II on each paper sample. To some extent, the fact
392 that the same donors provided natural marks along the study makes it possible to compare all
393 these scores and try figuring out some trends among the paper samples. Different
394 correlations with the detection quality scores were explored: vs porosity (Figure 13), vs
395 surface roughness (Figure 14), vs surface pH (Figure 15), and vs amount of carbonate lost
396 (Figure 16). It was indeed supposed that characteristics such as the paper porosity, the
397 surface roughness or the surface pH would play a direct role in the way SMD II behave
398 (detection quality and background). Also, given that a loss of calcium carbonate has been

399 observed, it appeared interesting to see if the modification of this layer may be correlated with
400 the SMD II performance.

401 < Insert Figure 13 here >

402 < Insert Figure 14 here >

403 < Insert Figure 15 here >

404 < Insert Figure 16 here >

405 When focusing on papers presenting no apparent issues in regards to fingerprint detection
406 (quality scores close to 3), it can be seen that the porosity is rather low, with average airflow
407 ranging from 0 to 1000 mL/min, the roughness is characterized by Rq values ranging from ca.
408 3 to 4 microns, the surface pH of the paper ranges from 4 to 7 and the loss of carbonate
409 ranges from ca. 30% to ca. 90%. However, papers leading to bad quality fingerprints (quality
410 scores close to 0) also present similar characteristics; their porosity is low to average, with
411 average airflow ranging from 0 to 1500 mL/min, the roughness is characterized by Rq values
412 ranging from ca. 2.5 to 4 microns, the surface pH ranges from 6 to 7, and the loss of
413 carbonate ranges from ca. 10% to 100%.

414 Therefore, from the analysis of Figures 13 to 15, no clear trends can be identified regarding
415 the quality of fingerprints in regards to porosity, surface roughness or surface pH of the
416 papers analyzed. The same observation is made with the loss of calcium carbonate.

417 About the surface pH, it can be noted that papers with acidic surface pH (below 6) led to no
418 zero quality scores, which means that SMD II was able to detect fingerprints for each of
419 them, but with varying quality levels. Beyond that observation, there seems to be no trend
420 between surface pH and SMD II performance. 85% of the paper samples are indeed
421 characterized by surface pH between 6 and 7, with quality scores ranging from 0 to 3.
422 Contrarily to what could be expected, an acidic surface pH is consequently not necessarily
423 associated with better detection quality.

424 From the analysis of some 3D topographies of the different types of samples, it is remarkable
425 that the same type of surface does not give the same quality of revelation of the fingerprints,

426 as it is for the C02 samples (quality score of 0.67) and C05 (quality score of 1.84). Illustrations
427 of processed paper samples bearing fingermarks are shown in Appendix B.

428 To further refine the analysis, statistical analysis was used to try and detect correlation
429 between background noise, fingermark quality and the paper variables. However, none of the
430 techniques used (Chi-square test, PCA, MCA and MLR) led to the detection of a correlation
431 between the parameters considered.

432 **3.5 General discussion**

433 Despite the number of different paper types collected, the various paper properties studied
434 and the large number of fingermarks processed with SMD II, no correlation between paper
435 properties and SMD II efficiency was highlighted. However, the chemical composition of the
436 surface coating is worth discussing further.

437 Regarding the experimental design, the number of donors has been voluntarily set low
438 because the study had not for aim to assess the intrinsic performance of SMD II as
439 fingermark detection technique. It rather aimed at studying the influence of paper samples on
440 its ability to detect fingermarks. Doing so requires limiting other influencing parameters, such
441 as the variability induced by donors and the age of the fingermarks. By choosing two average
442 donors, it was possible to assess how the performance of SMD II evolves when different
443 paper samples are considered. Increasing the number of donors would have not modified the
444 overall conclusions of the study and would have imply reducing the number of paper samples
445 to keep the quantity of fingermarks manageable.

446 Surface coating is made of silica or calcium carbonate. It is used to make the surface uniform
447 and improve the printing quality [22]. This coating is however soluble in acidic aqueous
448 solutions. Therefore, immersing the samples in colloidal gold will lead to its partial dissolution.
449 If the fingermark residue does not migrate deep enough in the layer of the paper [23], it will be
450 damaged. The dissolution of the fingermark may rely on two parameters: the thickness of the
451 coating layer and the depth of penetration in the paper. According to Vallette and Choudens
452 [22], and Santos et al. [24], the thickness of the coating is about 15 μm for paper of a weight
453 of 72 g/m^2 and more. It is also known that penetration depth depends on the paper type [23].
454 On coated papers, observed depth could be as deep as 30 μm . It means that even if the layer

455 is entirely removed, a fraction of the fingerprint residue may remain available for detection.
456 Uncoated papers contain calcium carbonate as well to improve their surface characteristics
457 and whiteness. This material may also be solubilised during SMD II processing and lead to
458 fingerprint degradation. Under these circumstances, the dynamic of diffusion of the secretion
459 residue into the substrates is expected to play a major role. Indeed, it could be hypothesized
460 that if the secretion residue has not migrated through the surface coating when the document
461 is processed by SMD II, its chance of being detected would be seriously reduced. The key
462 parameter to consider in a forthcoming study will be the aging time of the fingerprints, as we
463 made the choice to limit our study to one-month-old fingerprints for experimental reasons.
464 This observation is also compatible with another technique known to interact with the non-
465 water-soluble fraction of the secretion residue, that is, physical developer (PD). Previous
466 studies have shown that the performance of PD increases with the age of fingerprints [25].
467 Moreover, this technique requires an acid pre-treatment to neutralize the alkali filler particles
468 and to avoid an overall staining of the item. This appears compatible with the need for
469 secretion residue to penetrate the substrate beyond the filler/coating layers to have a chance
470 to be detected. Consequently, it may be interesting to correlate such conclusions with the
471 results of the present study, based on SMD II.

472 **4. Conclusions**

473 This study aimed at characterizing several paper types (e.g., surface composition, surface
474 pH, roughness and porosity) before and after the application of SMD II. Furthermore, we
475 investigated the possibility to correlate the measured parameters with the performance of
476 SMD II, in terms of ridge quality and background staining.

477 At the completion of this study, we were able to show that the following parameters show no
478 correlation with the SMD II performance: paper roughness, porosity and surface pH. IR
479 analysis showed that 81% of the papers are coated with carbonates and the thickness of this
480 layer varies from one sample to another. This layer appears to be solubilized during the SMD
481 II process. Since fingerprints are originally present at the surface of this coating, further
482 investigation should be carried out considering the correlation between the calcium carbonate
483 thickness and the SMD II detection performance. One hypothesis is that secretion residue
484 may migrate below the calcium carbonate layer if it is not too thick, and be further detected by
485 SMD II despite the dissolution of the carbonate-based coating. This hypothesis is worth being

486 further studied considering fingerprints of different ages. Moreover, it is expected that these
487 observations will be useful to physical developer as well.

488

489

490 **Table 1**

Parameter	Description	Formula
Ra	Arithmetic mean of absolute values of deviations y	$R_a = \frac{1}{n} \sum_{i=1}^n y_i $
Rq	Quadratic mean value of the profile deviations	$R_q = \sqrt{\frac{1}{n} \sum_{i=1}^n y_i ^2}$
Rt	Maximum Profile Height	$R_t = R_p - R_v$
Rz	The mean height difference between the 5 highest peaks and the 5 lowest valleys	$R_z = \frac{1}{5} \sum_{i=1}^5 R_{pi} - R_{vi}$

491

492 **Table 2**

Score	Qualitative observation
0	No ridge, no fingerprint visible
1	Ridges are visible over a small area (or over the whole mark), but it is extremely difficult to retrieve level II characteristics (such as minutiae) due to extremely poor ridge details.
2	Ridges are visible on almost the whole mark; level II characteristics can be retrieved. Nevertheless, the quality is not optimal due to a low contrast, strong background staining or faint ridges.
3	Ridges are very well defined on the whole mark. Level II characteristics can easily be retrieved. The contrast is optimal with no (or extremely faint) background staining.

493

494

495 **Table 3**

Frequency (cm ⁻¹)	Attribution
3332	O-H elongation with intramolecular
2897	CH ₂
1634	H ₂ O
1426	CH ₂ symmetrical deformation
1370	C-H deformation
1334	C-H shear (plane)
1316	CH ₂ agitation
1281	C-H deformation
1203	O-H deformation
1160	C-O and C-C elongation + CH ₂ rocking
1105	C-O and C-C elongation + CH ₂ rocking
1052	C-O elongation
1029	C-O elongation
1002	C-O and C-C elongation + CH ₂ rocking
897	Out-of-plane O-H deformation
659	Out-of-plane O-H deformation

496

497

498 **Table 4**

Frequency (cm ⁻¹)	Attribution
3700-3200	Si-OH
3360	H ₂ O absorbed
3000-2800	Organic C-H
1733, 1653, 1634	H ₂ O absorbed
1423	CH ₂ symmetrical deformation
1870-960	Vibrational network SiO ₂
1350-500	C-H vibration
1070	Si-O-Si symmetrical elongation
900-980	Free silanol elongation
800-820	Si-O-Si symmetrical elongation

499

500

501 **Figure captions**

- 502 Figure 1 Chemical structures of the major wood components: lignin (top), cellulose (bottom
503 left), and hemicellulose (bottom right) [12]
- 504 Figure 2 Example of treatment of the UV-Visible spectrum, from % Reflectance to log of
505 inverse reflectance allowing spectrum deconvolution, for the Staples Pastel (USA,
506 CO3). Red vertical line is λ_{max} , blue line is actual spectrum, green curves are the
507 resulting deconvoluted bands representing electronic transitions, and black
508 spectrum represent the result of the fitted deconvolution.
- 509 Figure 3 UV-Visible spectra of some of the analyzed paper samples. a) Kirkland Signature
510 (Mexico, C01), b) RetroPlus50 (Canada, C02), c) Esquisse envelope (France,
511 E21), d) Papyrus rainbow (Europe – unspecified country, E31).
- 512 Figure 4 Left half: 3D profiles of the RetroPlus50 (Canada; C02) and Staples Sustainable
513 Earth Copy Paper (USA; C05) paper samples after they were processed with SMD
514 II. Right half: illustration of the processed samples.
- 515 Figure 5 Average values of the Rq parameter (μm) for all the paper samples (see Appendix
516 A for manufacturer details).
- 517 Figure 6 Average air flow (mL/min) measured for all the paper samples (see Appendix A for
518 manufacturer details).
- 519 Figure 7 Chart illustrating the relation between the average airflow (mL/min) and the Rq
520 values (microns) for all the paper samples. Each dot represents a paper sample.
- 521 Figure 8 Top spectrum resulting from the subtraction of the IR spectra obtained before and
522 after the application of SMD II on the paper sample RetroPlus50 Canada (C02);
523 bottom IR spectrum corresponding to calcium carbonate.
- 524 Figure 9 Top spectrum obtained by subtracting the IR spectra obtained before (middle) and
525 after (bottom) the application of SMD II (paper sample: Kirkland Signature Mexico;
526 C01).

527 Figure 10 Difference spectra between C04 (top) and original C01 (bottom).

528 Figure 11 Infrared spectrum of the unprocessed Staples "Chemise à pochettes – 1336" paper
529 sample (C27).

530 Figure 12 Derivative calculation for the RetroPlus50 paper sample (Canada; C02). Top
531 spectra represent the paper surface with the fingermarks revealed, while bottom
532 spectra represent the opposite surface of the same paper.

533 Figure 13 Chart illustrating the relation between the airflow (mL/min) and the average quality
534 score associated with the fingermarks obtained after SMD II. Each dot represents a
535 paper sample.

536 Figure 14 Chart illustrating the relation between the Rq values (microns) and the average
537 quality score associated with the fingermarks obtained after SMD II. Each dot
538 represents a paper sample.

539 Figure 15 Chart illustrating the relation between the surface pH and the average quality score
540 associated with the fingermarks obtained after SMD II. Each dot represents a
541 paper sample.

542 Figure 16 Chart illustrating the relation between the calcium carbonate loss (estimated %)
543 and the average quality score associated with the fingermarks obtained after SMD
544 II. Each dot represents a paper sample.

545

546

547 **Table captions**

548 Table 1 Parameters Ra, Rq et Rz used to qualify paper surface roughness (n being the
549 number of peaks of the profile).

550 Table 2 Table used to assess the quality of the marks (reproduced from [16]).

551 Table 3 Main infrared peaks characteristic of cellulose in the majority of papers studied
552 **[Erreur ! Signet non défini.]**

553 Table 4 The main infrared peaks characteristic of the silicate gel [19,20,21]

554

555

556

557 **Competing statement**

558 The authors declare that they do not have any competing interest to declare.

559

560

561 **Funding**

562 The authors thank NSERC (National Sciences and Engineering Research Council of
563 Canada), FRQNT (Fonds de Recherche du Québec – Nature et Technologies) and CQMF
564 (Centre Québécois sur les matériaux fonctionnels, Gouvernement du Québec) for financial
565 support.

566

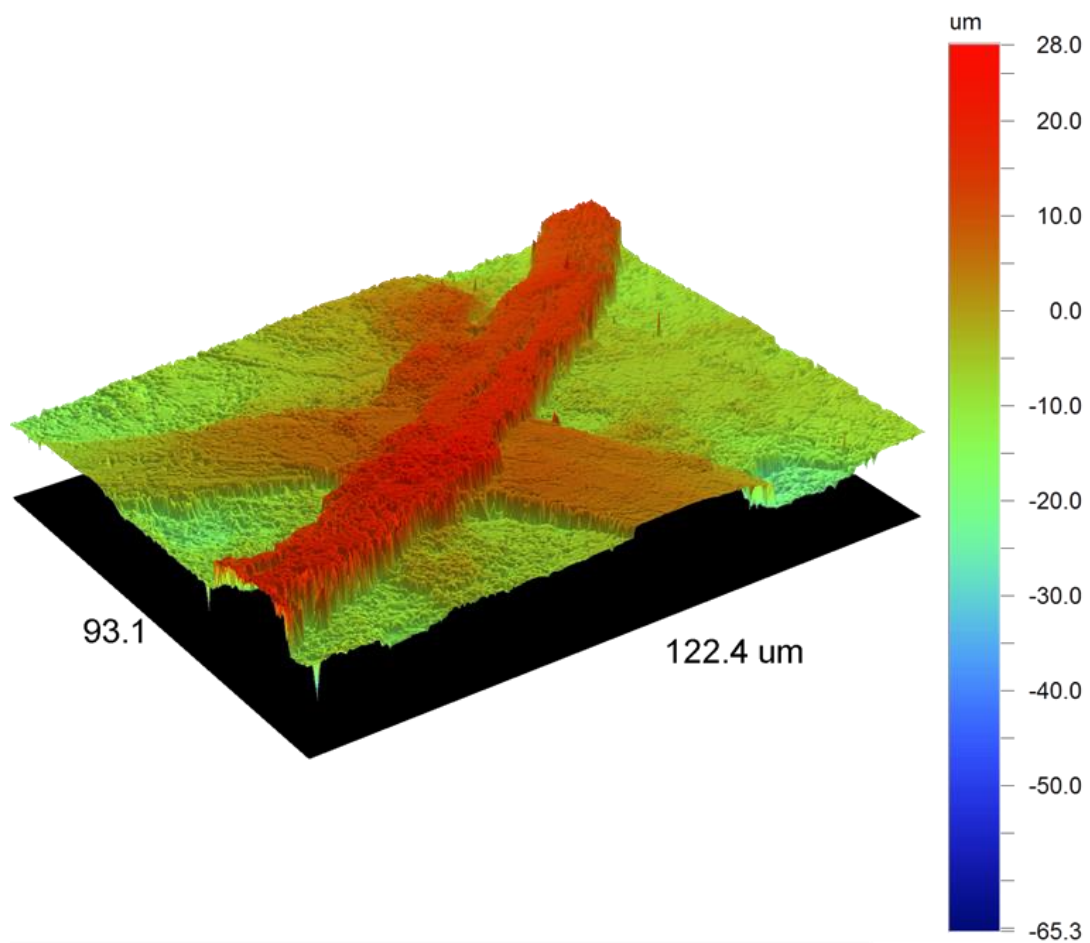
567

-
- 1 A. Bécue, S. Moret, C. Champod, P. Margot, Use of stains to detect fingerprints. *Biotech. Histochem*, **86**:3 (2011) 140-160. <https://doi.org/10.3109/10520290903462838>.
 - 2 G.C. Saunders, A.A. Cantu, *Universal Process for Fingerprint Detection*. Los Alamos National Laboratory Publication, **April** (1991).
 - 3 G.C. Saunders, Multimetal deposition method for latent fingerprint development. in 74th annual educational conference of the International Association for Identification. (1989). Pensacola, FL.
 - 4 B. Schnetz, P. Margot, Technical note: latent fingerprints, colloidal gold and multimetal deposition (MMD) - Optimisation of the method. *Forensic Sci. Int.*, **118**:1 (2001) 21-28. [https://doi.org/10.1016/S0379-0738\(00\)00361-3](https://doi.org/10.1016/S0379-0738(00)00361-3).
 - 5 E. Stauffer, A. Bécue, K.V. Singh, K.R. Thampi, C. Champod, P. Margot, Single-metal deposition (SMD) as a latent fingerprint enhancement technique: An alternative to multimetal deposition (MMD). *Forensic Sci. Int.*, **168**:1 (2007) e5-e9. <https://doi.org/10.1016/j.forsciint.2006.12.009>.
 - 6 P. Durussel, E. Stauffer, A. Bécue, C. Champod, and P. Margot, Single-Metal Deposition: Optimization of this Fingerprint Enhancement Technique. *J. For. Ident.*, 2009. **59**(1): p. 80-96. <https://doi.org/10.1016/j.forsciint.2006.12.009>.
 - 7 A. Bécue, A. Scoundrianos, S. Moret, Detection of Fingerprints by Colloidal Gold (MMD/SMD) - Beyond the pH 3 Limit. *Forensic Sci. Int.*, **219**:1-3 (2012) 39-49. <https://doi.org/10.1016/j.forsciint.2011.11.024>.
 - 8 S. Moret, A. Bécue, Single-Metal Deposition for Fingerprint Detection - A Simpler and More Efficient Protocol. *J. For. Ident.*, **65**:2 (2015) 118-137.
 - 9 C. Fairley, S.M. Bleay, V.G. Sears, N. Nic Daéid, A Comparison of Multi-metal Deposition Processes Utilising Gold Nanoparticles and an Evaluation of their Application to "Low Yield" Surfaces for Finger Mark Development. *Forensic Sci. Int.*, **217**:1-3 (2012) 5-18. <https://doi.org/10.1016/j.forsciint.2011.09.018>.
 - 10 T.G. Newland, S. Moret, A. Bécue, S.W. Lewis, Further investigations into the single metal deposition (SMD II) technique for the detection of latent fingerprints. *Forensic Sci. Int.*, **268** (2016) 62-72. <https://doi.org/10.1016/j.forsciint.2016.09.004>.
 - 11 C. Champod, C. Lennard, P. Margot, M. Stoilovic, *Fingerprints and Other Ridge Skin Impressions - Second Edition*. (2016), Boca Raton, Florida: CRC Press LLC. 427. ISBN 9781498728935.
 - 12 D.N.-S. Hon, N. Shiraishi, *Wood and Cellulosic Chemistry, Second Edition, Revised, and Expanded*, Marcel Decker Inc, New York, (2000), 928 Pages, ISBN 9780824700249.
 - 13 C. Antoine, Optimisation de l'état de surface des papiers supercalandrés (grade SCA) pour l'impression héliogravure, Master thesis, UQTR, (1996), URL: <http://depot-e.uqtr.ca/4657/1/000626161.pdf>

-
- 14 S. Adanur, Paper Machine Clothing: Key to the Paper Making Process, Technomic Publishing Company Inc., (1997). ISBN 1-56676-544-7.
 - 15 J.W. Martin, Concise Encyclopedia of the Structure of Materials, Elsevier Ltd, (2007). ISBN-10: 0-08-045127-6, ISBN-13: 978-0-08-045127-6.
 - 16 T. Fitzzi, R. Fischer, S. Moret, A. Bécue, Fingermark Detection on Thermal Papers: Proposition of an Updated Processing Sequence. *J. For. Ident.*, 64:4 (2014) 329-350.
 - 17 F.A. Miller, C.H. Wilkins, Infrared Spectra and Characteristic Frequencies of Inorganic Ions – Their Use in Qualitative Analysis, *Anal. Chem.*, 24:8 (1952) 1253-1294. <https://doi.org/10.1021/ac60068a007>.
 - 18 Svanholm, Erik., Printability and Ink-coating Interactions in Inkjet Printing, Karlstad University Studies, (2007). ISBN 91-7063-104-2.
 - 19 G. Socrates, Infrared and Raman Characteristic Group Frequencies Tables and Charts, Third Edition, John Willey & Sons, LTD, New York, (2001). ISBN: 978-0-470-09307-8.
 - 20 R.F.S. Lenza, W.L. Vasconcelos, Preparation of Silica by Sol-Gel Method Using Formamide, *Mat. Res.*, 4:3 (2001). <https://doi.org/10.1590/S1516-14392001000300008>.
 - 21 A.M. Putz, M. Putz, Spectral Inverse Quantum (Spectral-IQ) Method for Modeling Mesoporous Systems: Application on Silica Films by FTIR, *Int. J. Mol. Sci.* 13 (2012) 15925-15941. <https://doi.org/10.3390/ijms131215925>.
 - 22 P. Vallette, C. Choudens, Le Bois, la Pâte, le Papier, deuxième édition, Centre Technique de l'Industrie des Papiers, Cartons et Celluloses, 1989.
 - 23 J. Almog, M. Azoury, Y. Elmaliah, L. Berenstein, A. Zaban, "Fingerprint's third dimension: The depth and shape of fingerprints penetration into paper - Cross section examination by fluorescence microscopy", *J. Forensic Sci.* 2004;49(5):981-985
 - 24 N.F. Santos, J. Velho, C. Gomes, Influence of calcium carbonate coating blends upon paper properties, Congreso iberoamericano de investigacion en celulosa y papel, 2000.
 - 25 J. Salama, S. Aumeer-Donovan, C. Lennard, C. Roux, Evaluation of the fingermark reagent Oil red O as a possible replacement for physical developer, *J. For. Ident.*, 58:2 (2008) 203-237.

Figures

Graphical Abstract (1328 x 531 pixels at 96 dpi)



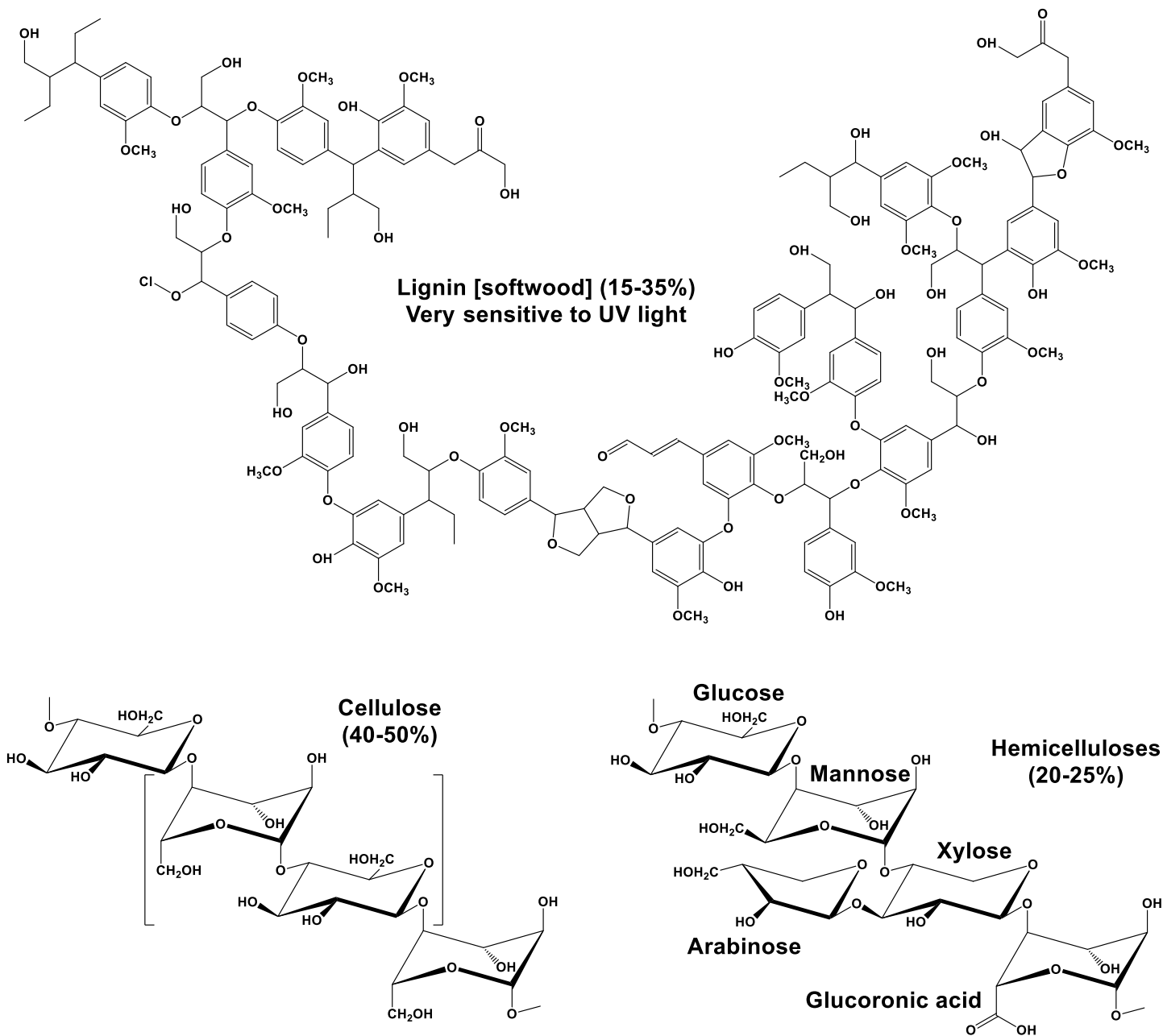


Figure Erreur ! Document principal seulement. Chemical structures of the major wood components: lignin (top), cellulose (bottom left), and hemicellulose (bottom right) [12]

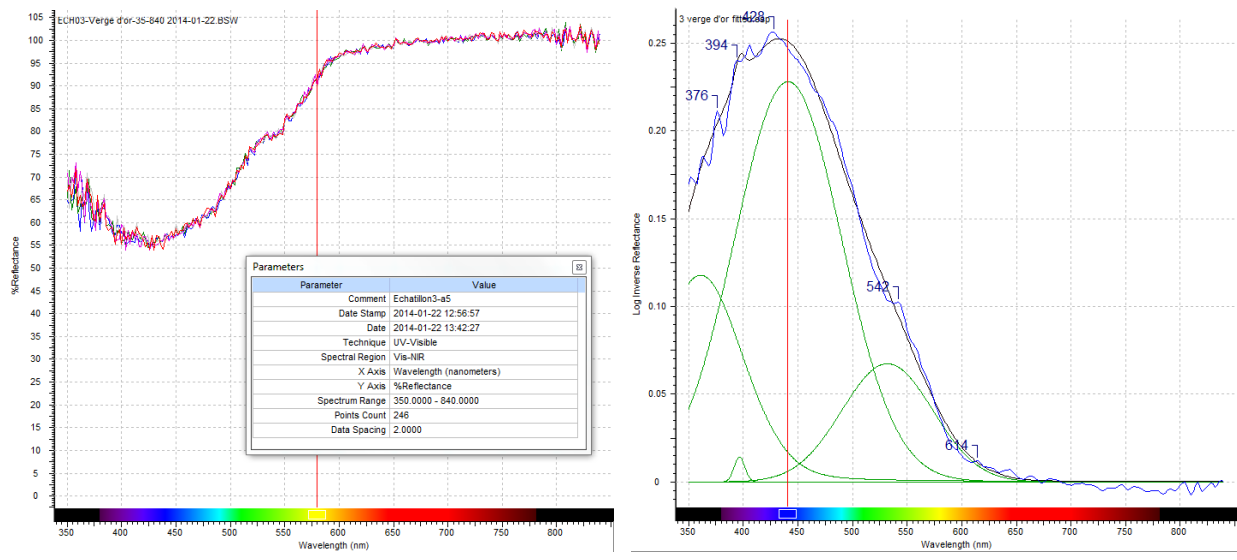


Figure Erreur ! Document principal seulement. Example of treatment of the UV-Visible spectrum, from % Reflectance to log of inverse reflectance allowing spectrum deconvolution, for the Staples Pastel (USA, CO3). Red vertical line is λ_{max} , blue line is actual spectrum, green curves are the resulting deconvoluted bands representing electronic transitions, and black spectrum represent the result of the fitted deconvolution.

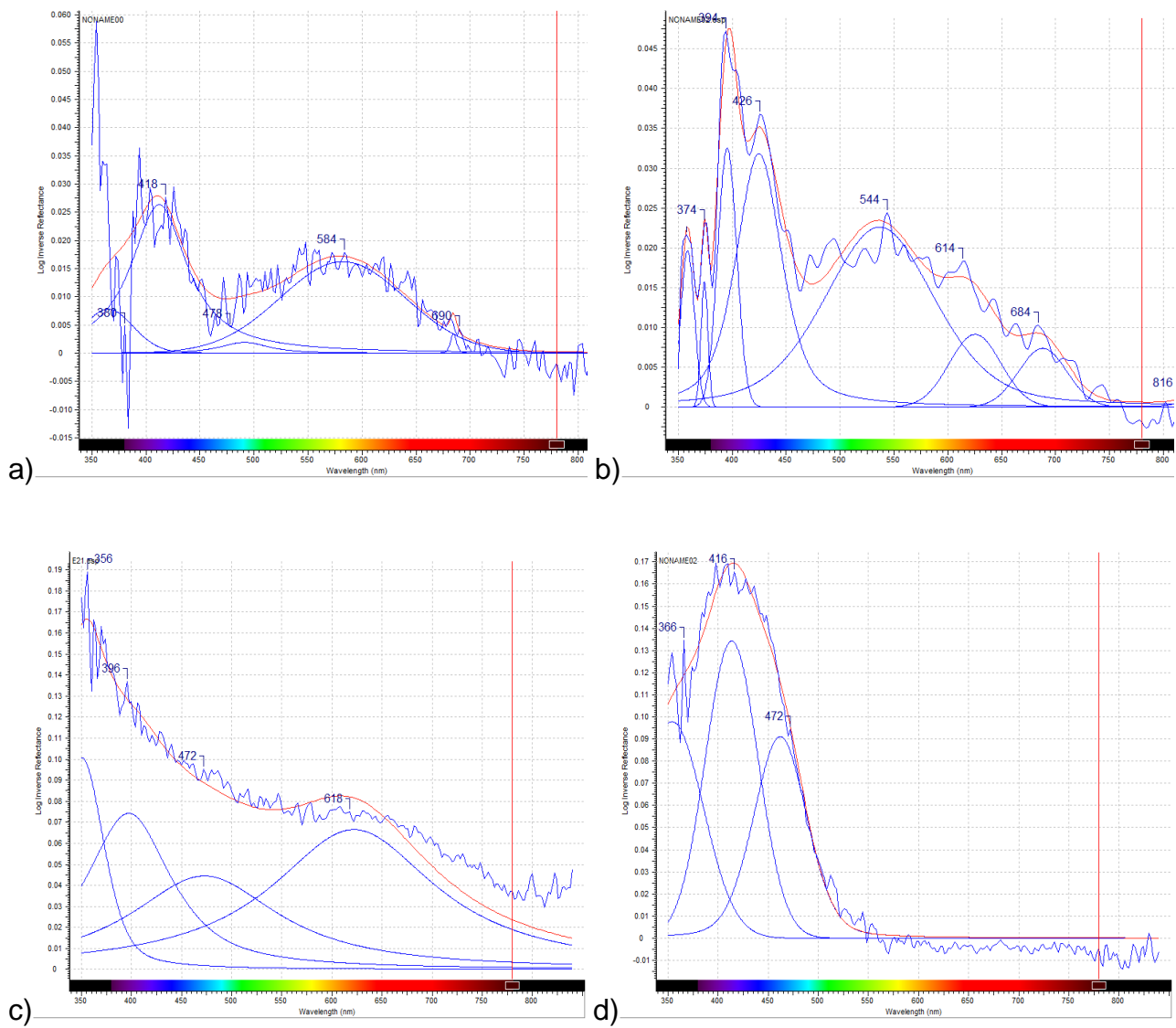


Figure Erreur ! Document principal seulement. UV-Visible spectra of some of the analyzed paper samples. a) Kirkland Signature (Mexico, C01), b) RetroPlus50 (Canada, C02), c) Esquisse envelope (France, E21), d) Papyrus rainbow (Europe – unspecified country, E31).

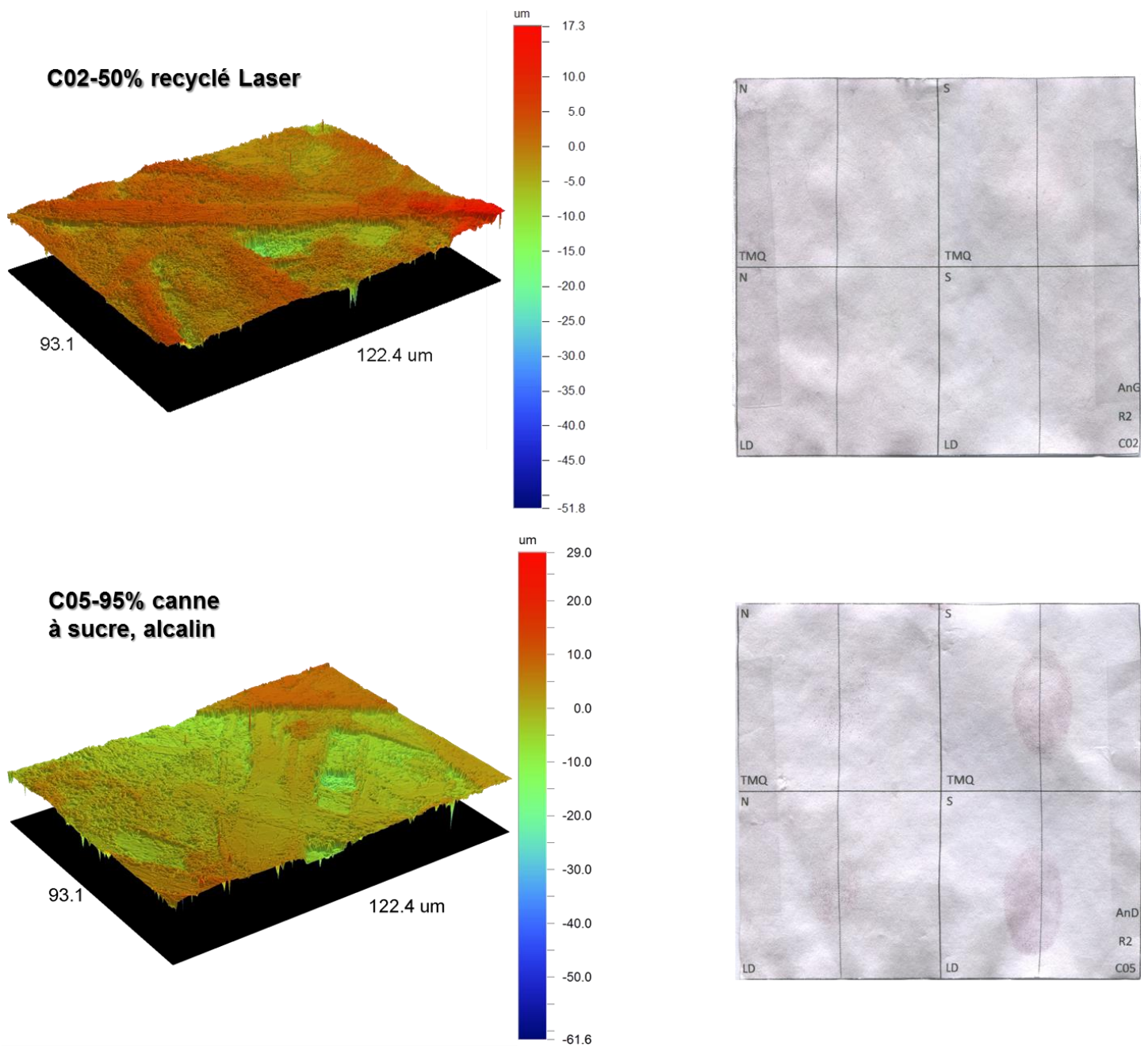


Figure 4 Left half: 3D profiles of the RetroPlus50 (Canada; C02) and Staples Sustainable Earth Copy Paper (USA; C05) paper samples after they were processed with SMD II. Right half: illustration of the processed samples.

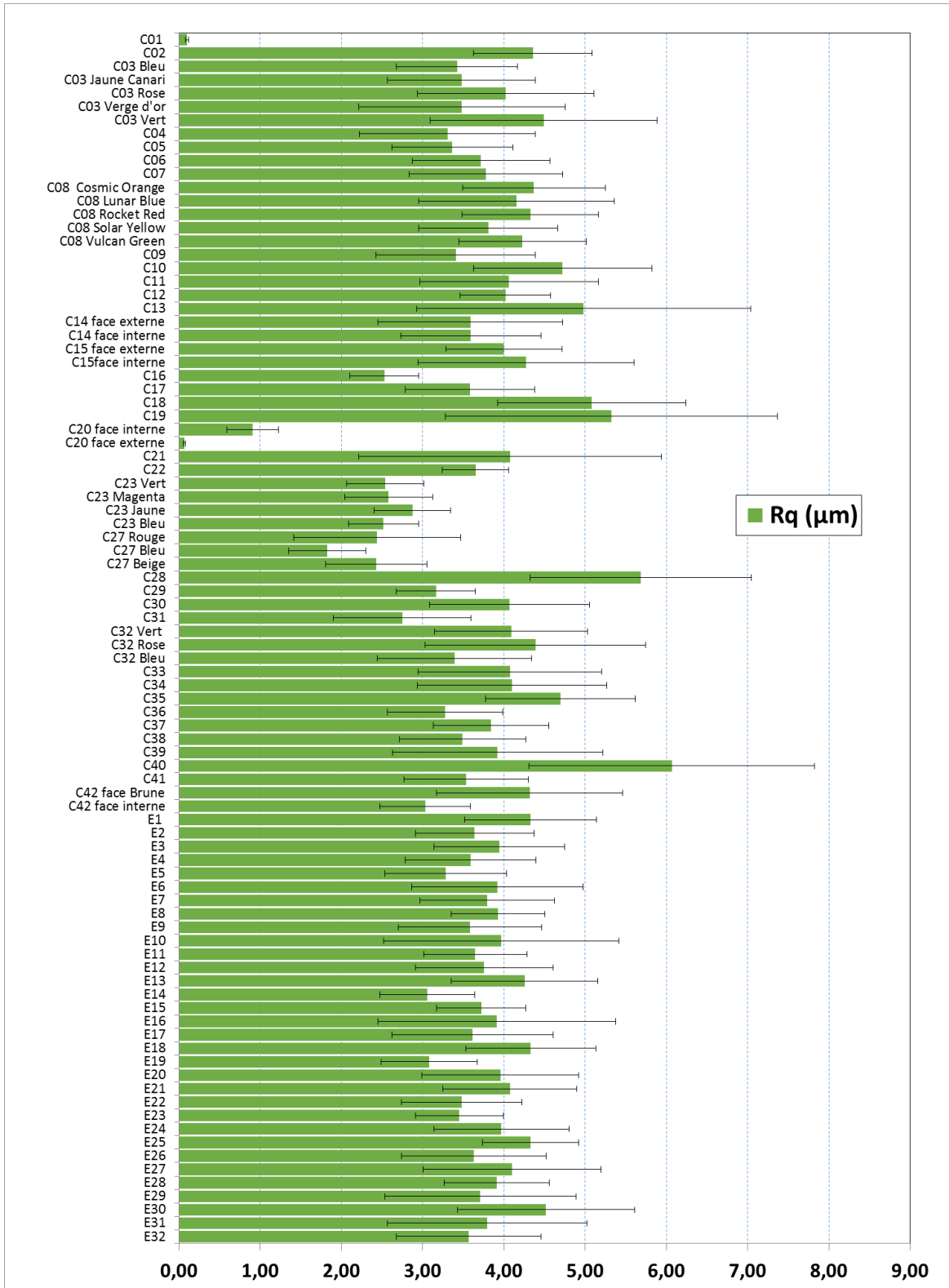


Figure 5 Average values of the Rq parameter (µm) for all the paper samples (see Appendix A for manufacturer details).

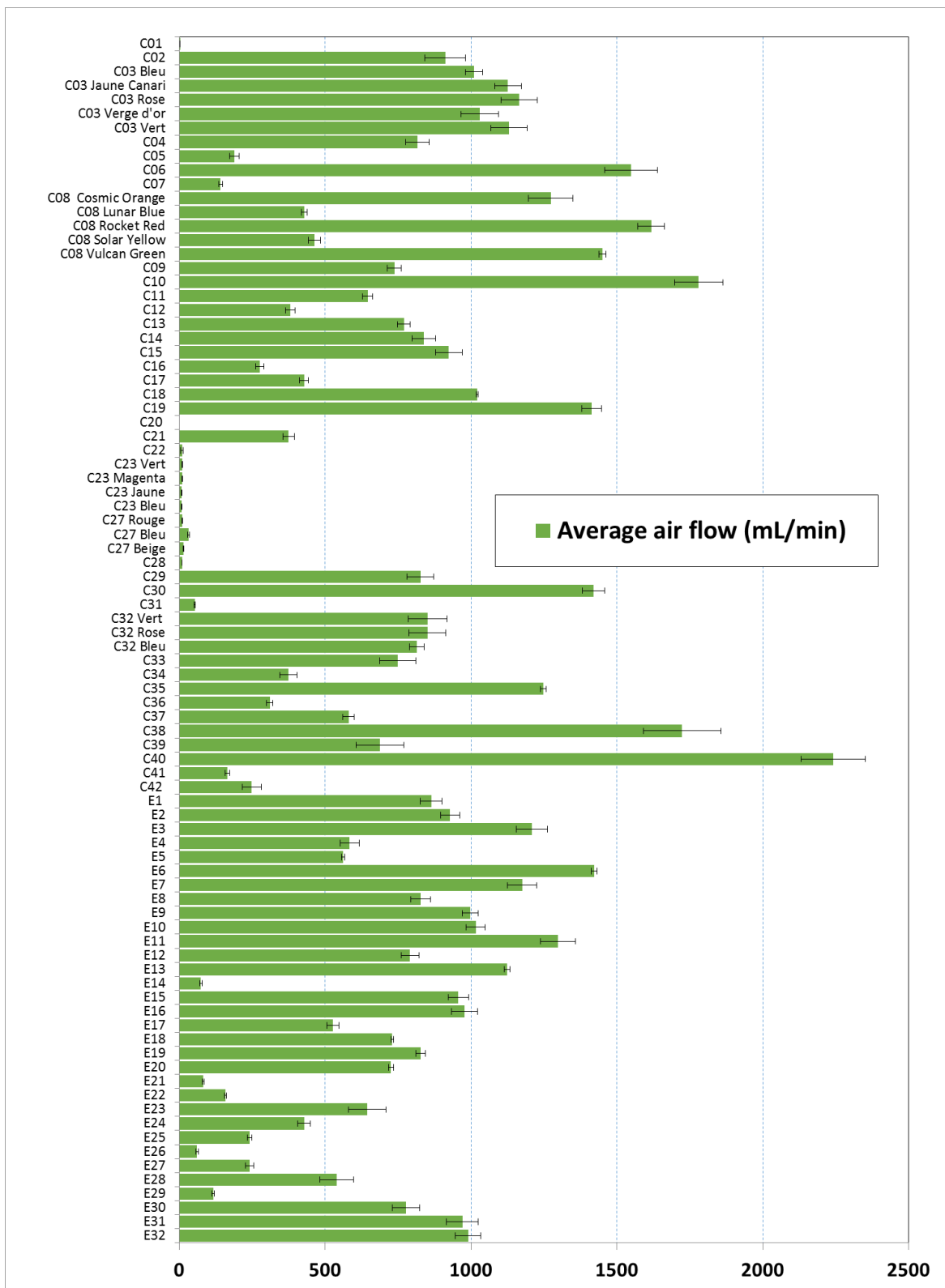


Figure 6 Average air flow (mL/min) measured for all the paper samples (see Appendix A for manufacturer details).

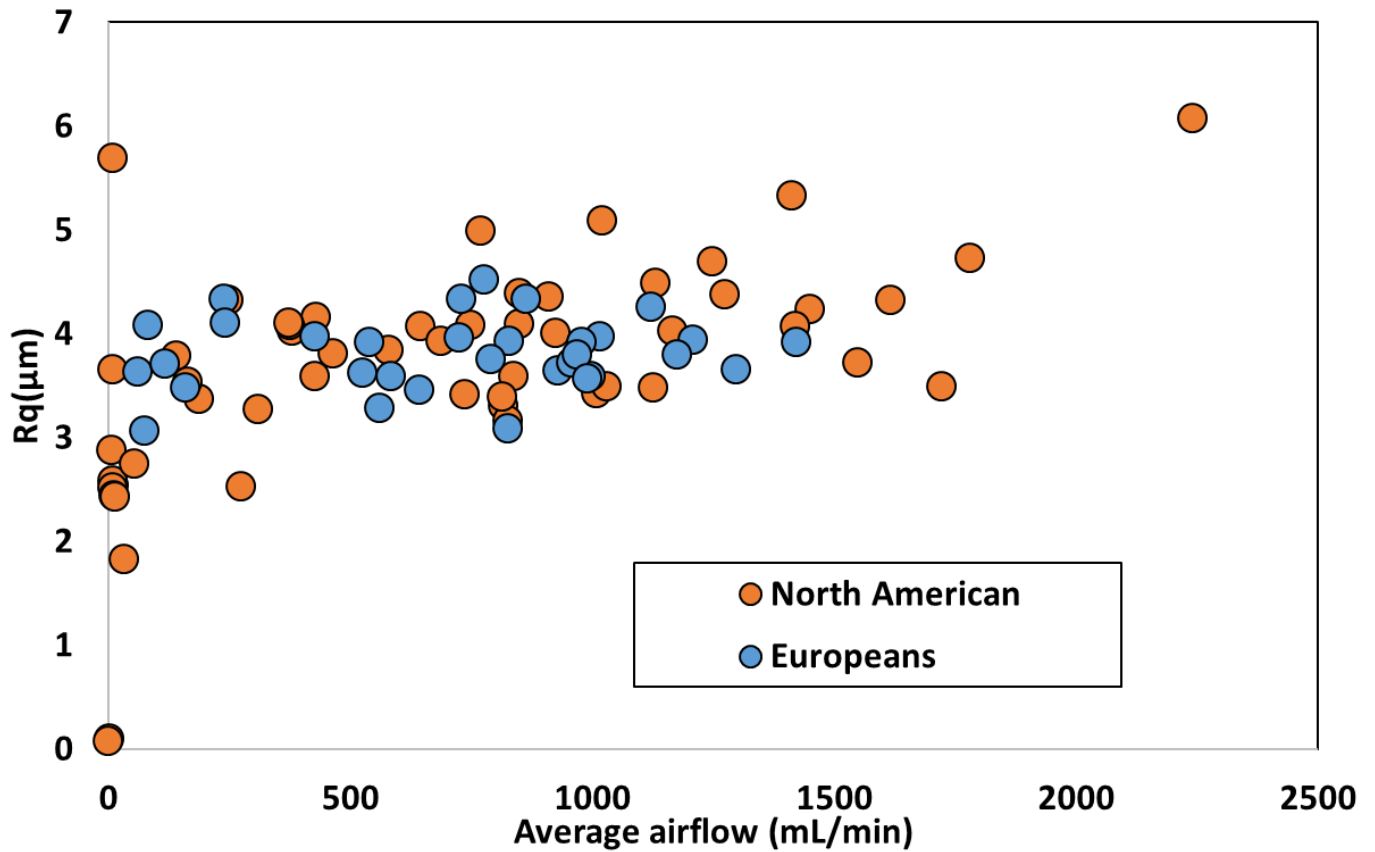


Figure 7 Chart illustrating the relation between the average airflow (mL/min) and the Rq values (microns) for all the paper samples. Each dot represents a paper sample.

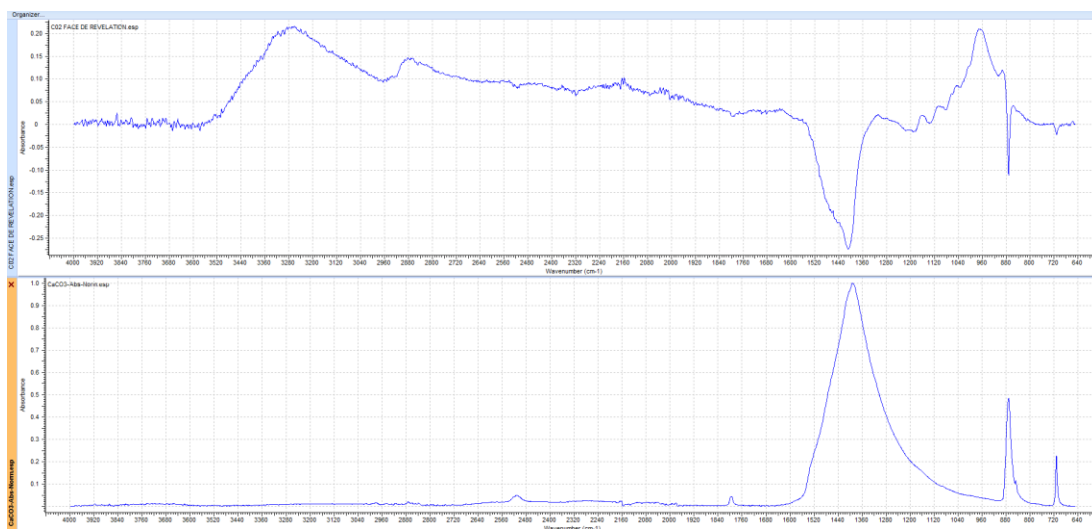


Figure 8 Top spectrum resulting from the subtraction of the IR spectra obtained before and after the application of SMD II on the paper sample RetroPlus50 Canada (CO₂); bottom IR spectrum corresponding to calcium carbonate.

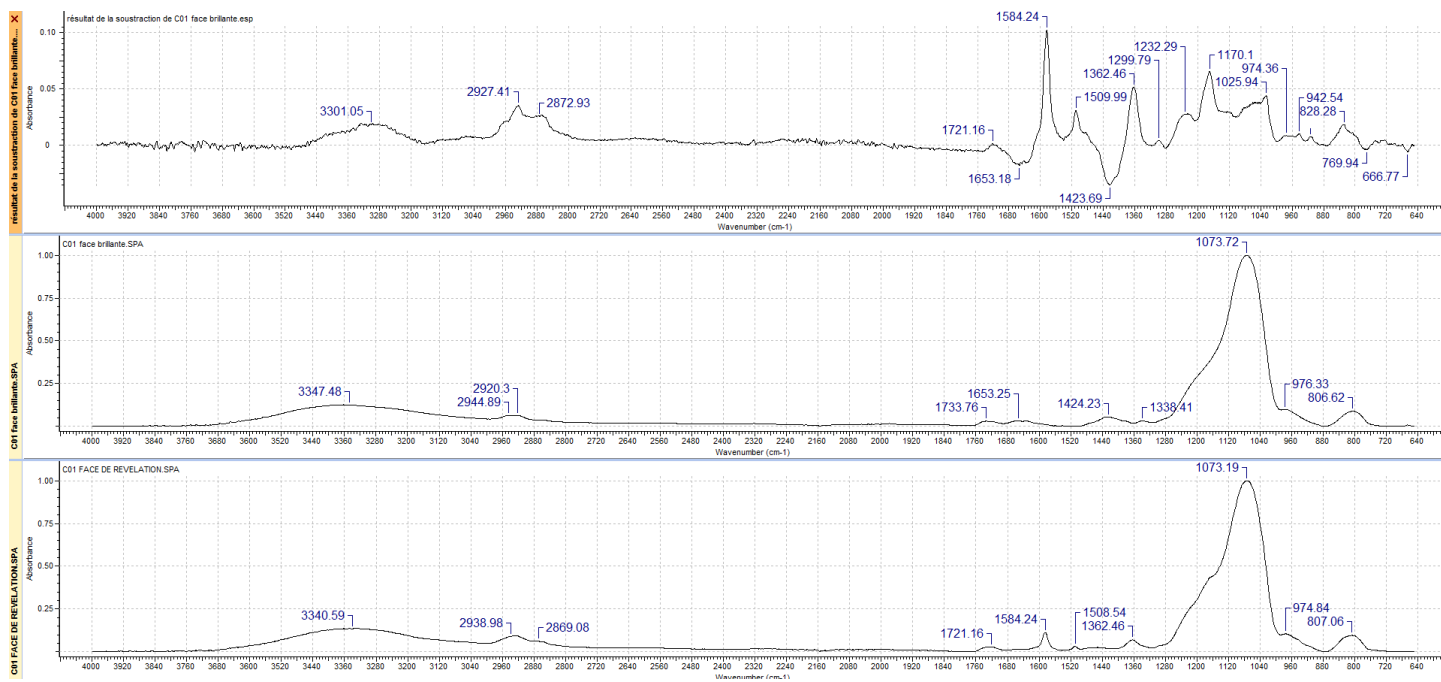


Figure 9 Top spectrum obtained by subtracting the IR spectra obtained before (middle) and after (bottom) the application of SMD II (paper sample: Kirkland Signature Mexico; C01).

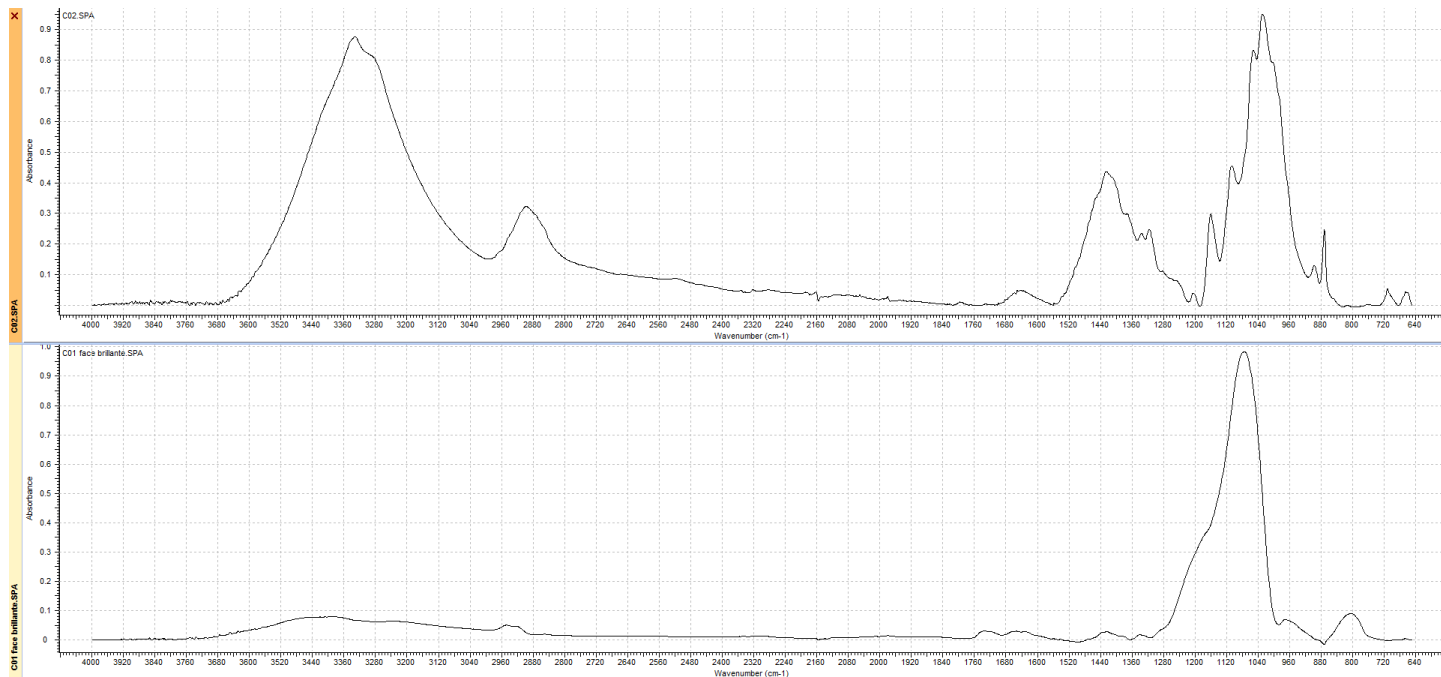


Figure 10 Difference spectra between C04 (top) and original C01 (bottom).

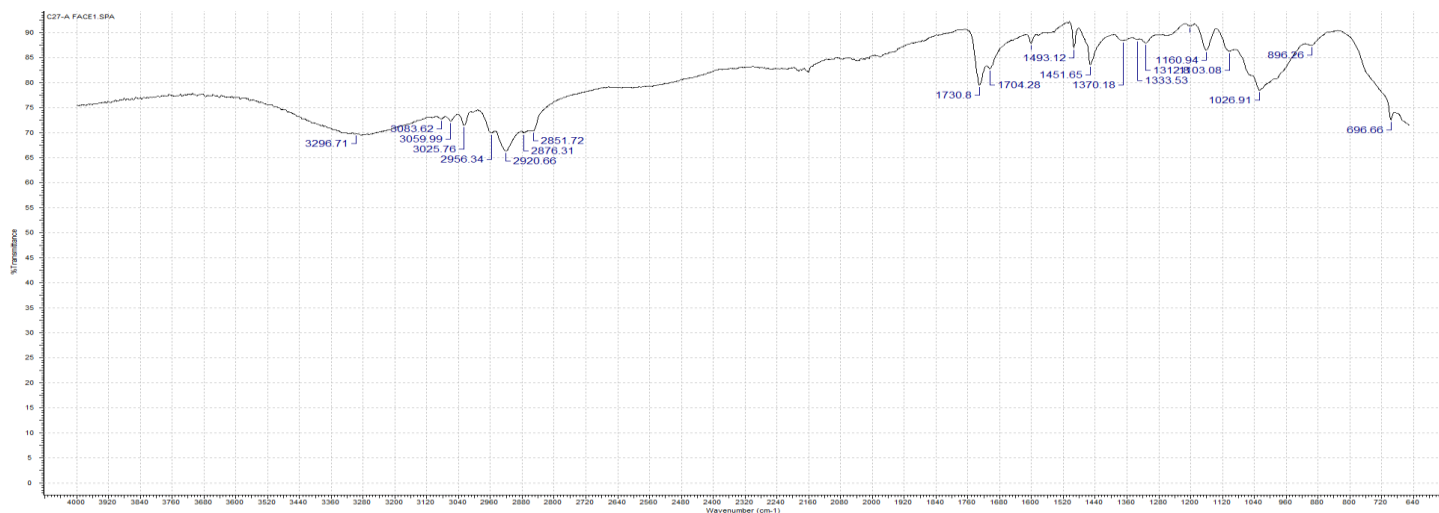


Figure 11 Infrared spectrum of the unprocessed Staples "Chemise à pochettes – 1336" paper sample (C27).

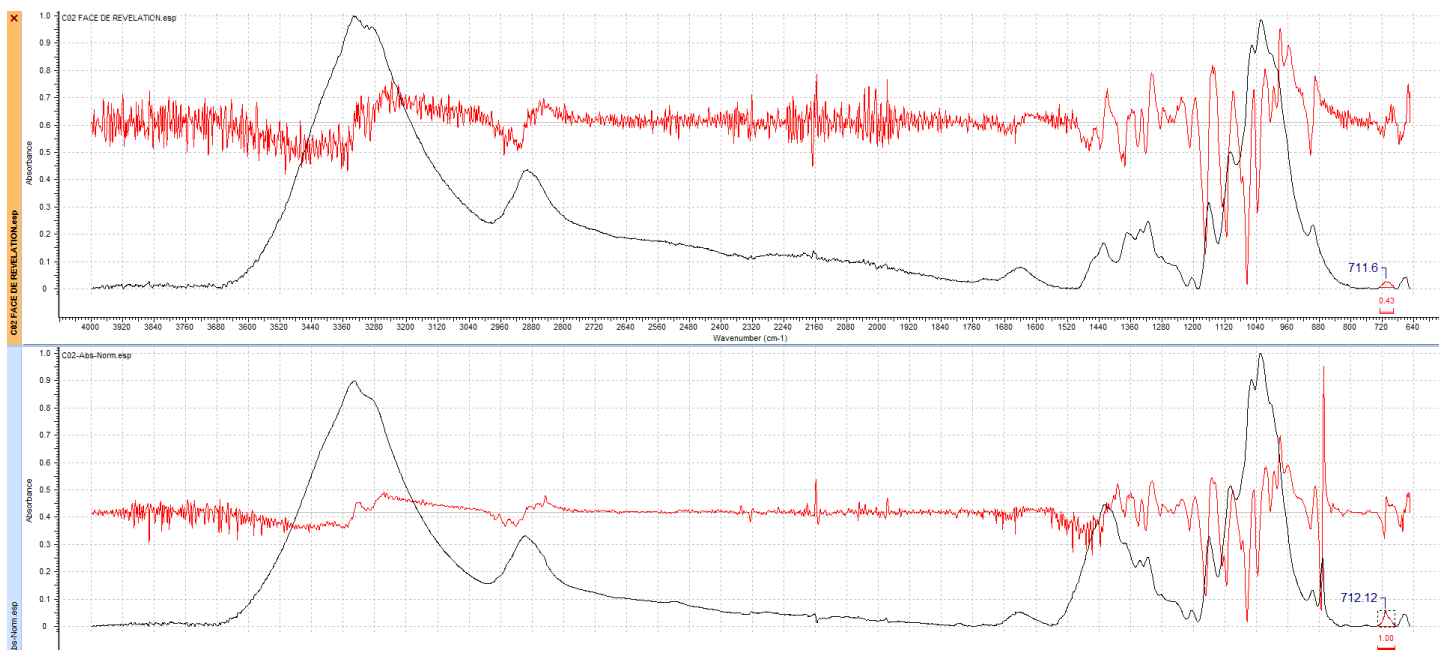


Figure 12 Derivative calculation for the RetroPlus50 paper sample (Canada; C02). Top spectra represent the paper surface with the fingermarks revealed, while bottom spectra represent the opposite surface of the same paper.

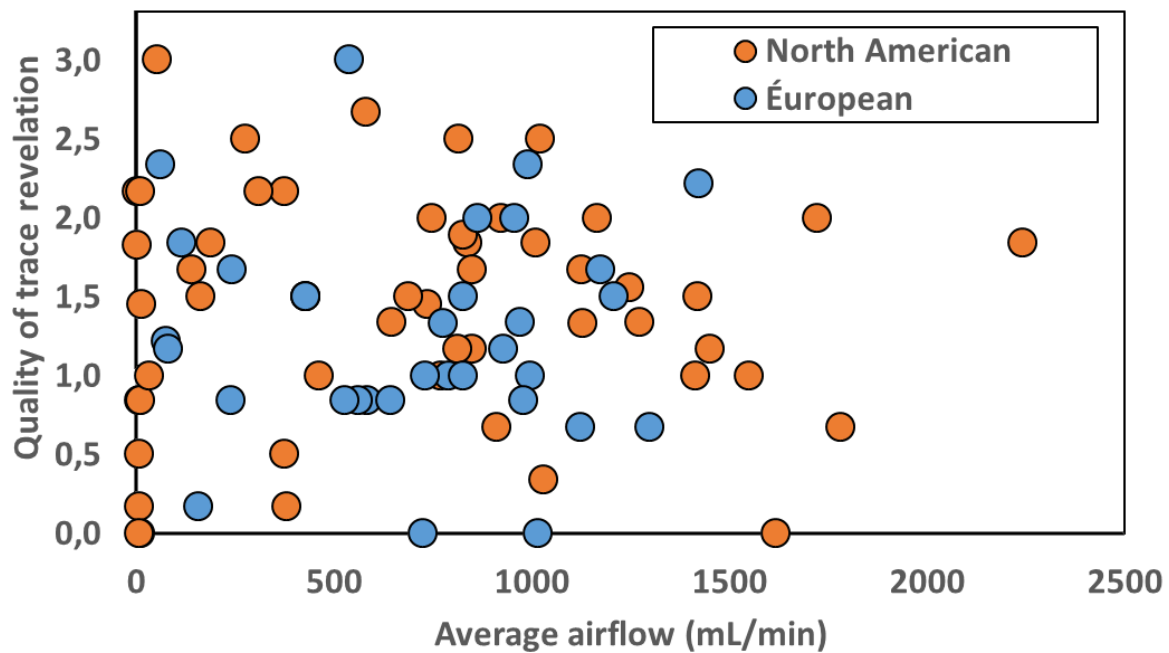


Figure 13 Chart illustrating the relation between the airflow (mL/min) and the average quality score associated with the fingermarks obtained after SMD II. Each dot represents a paper sample.

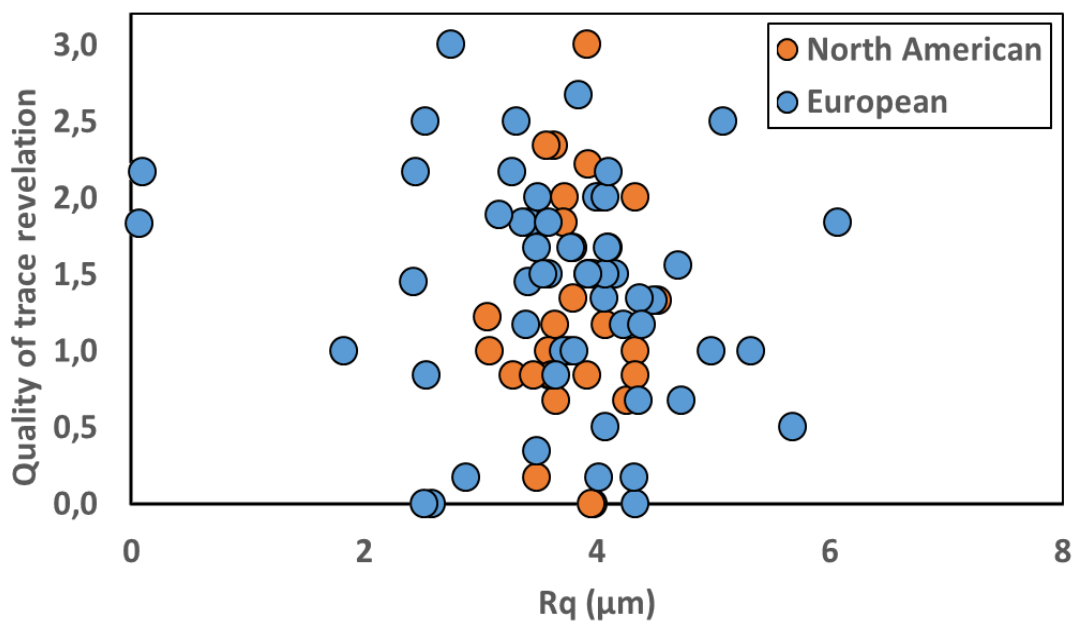


Figure *Erreur ! Document principal seulement.* Chart illustrating the relation between the Rq values (microns) and the average quality score associated with the fingermarks obtained after SMD II. Each dot represents a paper sample.

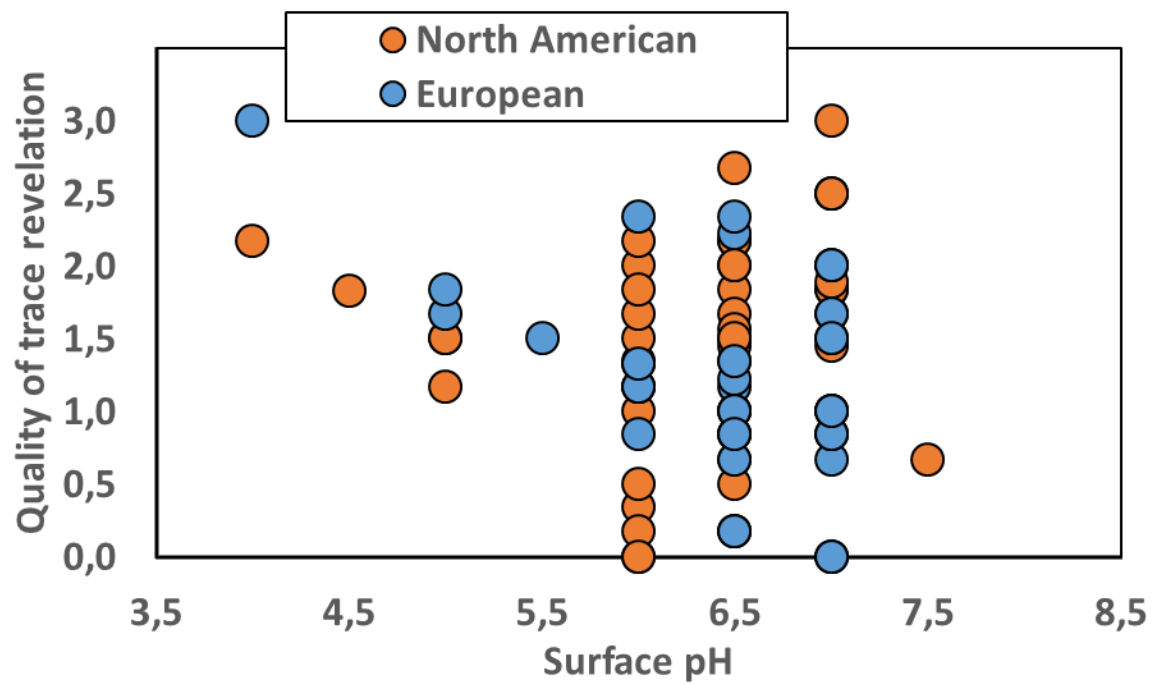


Figure *Erreur ! Document principal seulement.* Chart illustrating the relation between the surface pH and the average quality score associated with the fingermarks obtained after SMD II. Each dot represents a paper sample.

